ภาคผนวก

เอกสารการตีพิมพ์เผยแพร่และนำเสนอผลงานวิจัย

Carbohydrate Polymers 89 (2012) 251–258

Contents lists available at SciVerse ScienceDirect

Carbohydrate Polymers

journal homepage: www.elsevier.com/locate/carbpol

Green natural rubber-g-modified starch for controlling urea release

Sa-Ad Riyajan[a,*], Yodsathorn Sasithornsonti[a,1], Pranee Phinyocheep[b]

[a] Department of Materials Science and Technology and Natural Products Research Center, Faculty of Science, Prince of Songkla University, Songkhla 90110, Thailand
[b] Department of Chemistry, Faculty of Science, Mahidol University, Rama VI, Bangkok 10400, Thailand

ARTICLE INFO

Article history:
Received 17 December 2011
Received in revised form 28 January 2012
Accepted 1 March 2012
Available online 7 March 2012

Keywords:
Natural rubber
Starch
Grafting
Encapsulation
Fertilizer

ABSTRACT

The hydrophilicity of natural rubber (NR) was improved by grafting with modified cassava starch (ST) (NR-g-ST) by using potassium persulfate ($K_2S_2O_8$) as a catalyst. The modified ST was added to NR latex in the presence of Terric16A16 as a non-ionic surfactant at 60 °C for 3 h and cast film on a glass plate to obtain NR-g-ST. The chemical structure of NR-g-ST was confirmed by FTIR. The swelling ratio of NR-g-ST was investigated in water and results showed that the swelling ratio of the modified NR decreased as function of ST. In addition, the tensile strength of the modified NR in the presence of modified ST at 50 phr was the highest value. Also, the thermal stability modified NR-g-ST was higher than of NR/ST blend confirmed by TGA. Finally, the NR-g-ST was used a polymer membrane for controlling urea fertilizer and it easily degraded in soil. This product with good controlled-release and water-retention could be especially useful in agricultural and horticultural applications.

Published by Elsevier Ltd.

1. Introduction

Natural rubber (NR) containing 93–95% *cis*-1,4-polyisoprene is an elastomeric material, which produces from latex of the rubber tree. NR, as a renewable natural resource, has many excellent comprehensive properties such as outstanding resilience, and high strength. However, as an unsaturated polymer, NR will gradually degrade at a high temperature or when exposed to oxygen, ozone or ultraviolet, leading to a portentous negative effect on its special application (Agarwal, Setua, & Sekha, 2005; Chaikumpollert et al., 2011; Pasquini, Teixeira, Curvelo, Belgacem, & Dufresne, 2010; Zou et al., 2001). To overcome these limitations of NR, the modification of NR is crucial. Various methods can be employed to modify the properties of NR. One way is chemical modification, in which other groups or atoms are introduced onto the NR molecular chains, for example, epoxidized NR (Gan & Hamid, 1997; Yu, Zeng, Lu, & Wang, 2008), hydrogenated NR (Mahittikul, Prasassarakich, & Rempel, 2009), and grafted NR (Abu Bakar, Ismail, & Abu Bakar, 2010; Derouet, Intharapat, Tran, Gohier, & Nakason, 2009; Kongparakul, Prasassarakich, & Rempel 2008).

From previous work, the NR was modified by grafting with dimethylaminoethyl methacrylate (DMAEMA) to form a latex with cationic water-soluble polymeric 'hairs' of polyDMAEMA. They acted as filler in the starch (ST) films, but with modified NR, the mechanical properties of the films were significantly altered (Rouilly, Rigal, & Gilbert, 2004). The elastic modulus was greatly decreased but strain at break greatly increased. Freeze-fracture TEM micrographs indicate strong interactions between the surface of the modified NR and ST. The polyDMAEMA chains are more hydrophilic than the ST, and the addition of grafted latex results in a 20° drop of the water contact angle of the formed film and a 25% increase of the water absorption compared to the native ST; with unmodified NR, causes the opposite effect. Moreover, the properties of NR were improved by blending with ST. For example, thermoplastic ST/NR polymer blends were obtained using NR latex and cornstarch and an intensive batch mixer at 150 °C, with NR content varying from 2.5 to 20% (Carvalhoa, Jobb, Alvesb, Curveloa, & Gandini, 2003). The results revealed a reduction in the modulus and in tensile strength; the blends became less brittle than thermoplastic starch alone. Increasing plasticizer content made higher amounts of rubber possible. The addition of rubber was, however, limited by phase separation the appearance of which depended on the glycerol content. After ST paste (MST) modified with polybutylacrylate (PBA), it was used as a reinforcing filler of rubber through mixing and co-coagulating with NR latex (Liu, Shao, & Jia, 2008). MST is much superior to unmodified ST paste because unmodified ST paste acts as an essential inert filler causing a decrease in tensile strength, tear strength and elongation at break. MST shows an obvious reinforcement for NR matrix observed from increasing mechanical properties. Moreover, fine ST dispersion and strong interfacial interaction are achieved in NR/MST composites (Liu et al., 2008). Recently, NR was used to improve the properties of ST foam by potassium persulfate as an initiator (Tanrattanakul & Chumeka, 2010). In this work, NR was grafted with modified cassava

* Corresponding author. Tel.: +66 74888361; fax: +66 74446925.
E-mail address: saadriyajan@hotmail.com (S.-A. Riyajan).
[1] Tel.: +66 74888361; fax: +66 74446925.

0144-8617/$ – see front matter. Published by Elsevier Ltd.
doi:10.1016/j.carbpol.2012.03.004

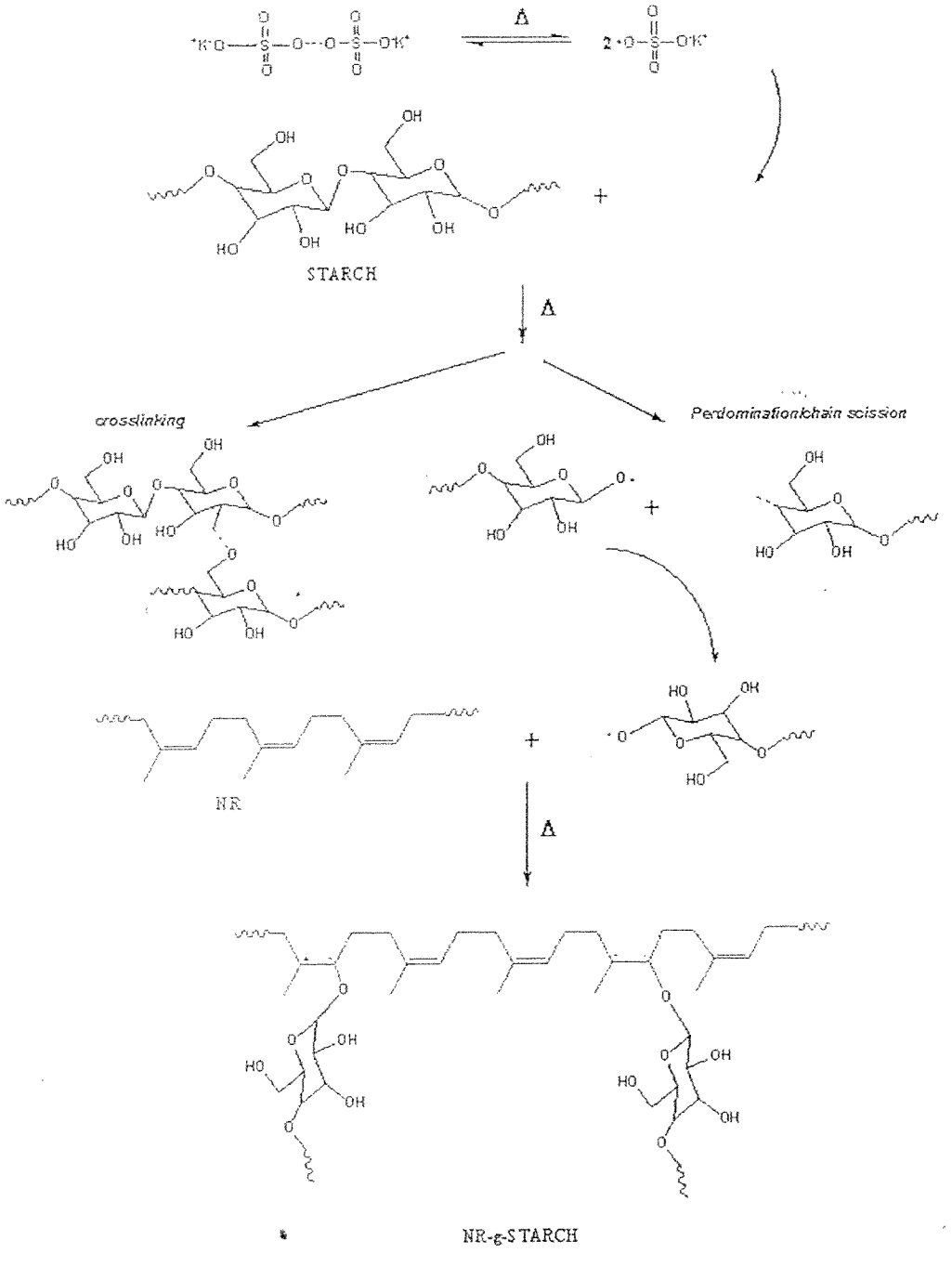

Fig. 1. The possible chemical reaction of NR-g-ST by using potassium persulfate as a catalyst.

the initiator concentration on graft copolymerization was studied at various $K_2S_2O_8$ concentrations by keeping other reaction conditions constant. it was found that the $K_2S_2O_8$ would destroy the structure of NR molecules. This result supports the previous work (Riyajan, 2007).

The synthesized copolymers were characterized by the functional groups using ATR-FTIR technique. ATR-FTIR spectra of unmodified ST and modified ST are presented in Fig. 2(A). The absorbent band of hydroxyl group was observed at 3340 cm^{-1}. The absorption at 879 cm^{-1} was referred to a methane vibration and

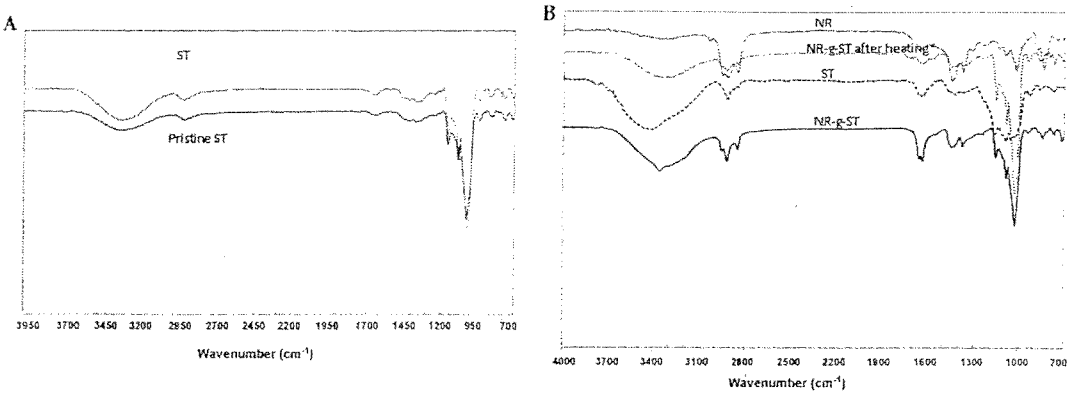

Fig. 2. ATR-FTIR spectra of ST and modified ST (B) NR, ST, NR-g-ST before and after THF extractions for 48 h and NR-g-ST after heating from 50 to 300 C by TGA.

absorption at 1638 cm^{-1} is C—O vibrations in ST. The vibrations of unsymmetry C—O—C bond and C—O bond in ST are at 1154 cm^{-1} and 1045 cm^{-1}, respectively (Rouilly et al., 2004). After chemical modification of the ST with $K_2S_2O_8$, the FTIR peak band was slightly altered as shown Fig. 2(A). The FTIR spectra for ST, NR-g-ST before and after THF extractions for 48 h are presented in Fig. 2(B). The results showed that the main FTIR band of ST was observed at 3550–3200, 2933 cm^{-1} and the two band of 1155, and 1080 cm^{-1} for hydroxyl group, the C—H stretching and the C—O—C stretching (a triplet peak of ST), respectively. The C—H stretching at 2965, 2928 cm^{-1}, the C=CH stretching at 1659 cm^{-1}, the $-CH_3$ deformation at 1452 cm^{-1}, the $-CH_2$ deformation at 1379 cm^{-1} and the C=CH bending at 843 cm^{-1} of NR-g-ST appeared in the FTIR spectra (Fig. 2(B)). The chemical structure of NR-g-ST was confirmed again by both TGA and FTIR. After NR-g-ST was heated from 50 to 330 °C by TGA technique, then its chemical structure was continually characterized by FTIR. It was clear that the notable difference between the FTIR spectra of ST and NR-g-ST was that the strongest peak for NR-g-ST appeared at 1100 cm^{-1} (C—O—C) comparing to ST. This data indicated that NR was grafted with ST. In addition, the thermal stability of NR-g-ST was the highest comparing other samples (see in Section 3.4). These results agreed with works of Tanrattanakul and Chumeka (2010). They studied the preparation of thermoplastic starch foams from pristine cassava starch blended with NR latex by reactive blending and potassium persulfate as an initiator for graft copolymerization between the ST and NR during baking. The chemical structure of NR-g-ST was confirmed by ^1H NMR and FTIR characterization. In case of FTIR, it was found a trace of an NR component in NR-g-ST (this subtracted spectrum before and after Soxhlet extraction) as appeared at 2926–2854 cm^{-1}.

3.2. Swelling behavior and mechanical strength

The swelling ratio of the modified NR is shown in Fig. 3(A). The swelling ratio of NR/ST blend without $K_2S_2O_8$ showed the highest value compared to other samples due to the absence of chemical interaction between ST and NR. When NR/ST blend was immersed in water for 2 days, the swelling ratio of the NR/ST increased from 160 to 180%.

But after 2 days, the swelling ratio of NR/ST decreased as a function time due to solubility of ST in NR/ST. After adding $K_2S_2O_8$ in polymer blend, the swelling ratio of NR-g-ST was dramatically decreased due to grafting with ST on molecule of NR. When over 50 phr ST was added, the swelling ratio of NR-g-ST increased with increasing ST contents due to its hydrophilic ST. The highest swelling ratio was observed in sample in the presence of 150 phr ST. This explains that excess ST exhibits good water solubility and leads to excellent swelling ratio in water.

The effect of modified ST on the tensile strength of NR-g-ST is presented in Fig. 3(B). The tensile strength of NR-g-ST increased as a function of modified ST contents in sample at range from 25 to 50 phr of ST. The highest tensile strength of the modified ST was found to be in sample in the presence of 50 phr ST and its tensile strength was about 6.8 MPa. But when the amount of ST was increased from 50 to 100 or 150 phr, tensile strength of modified ST decreased from 6.8 to 4.5 (3.5) MPa, respectively. Fig. 3(C) shows the elongation at break of the modified NR. Results showed that the elongation at break of the NR was about 900% while the elongation at break of modified ST in the presence of 25 phr was 950%. When ST was over 25 phr, the elongation at break the modified NR was dramatically decreased due to difference in polarity between NR and ST (Rouilly et al., 2004).

3.3. Morphology

SEM was used to change the morphology of NR/ST blend and NR-g-ST by $K_2S_2O_8$ as a catalyst as shown in Fig. 4. It was observed that the polymer blend (Fig. 4(A)) showed the poor adhesion between NR and ST. The larger ST part (light-gray areas) was poor dispersed in NR/ST matrix (dark-gray areas). In addition, the ST part phase was separated from the polymer matrix because NR is hydrophobic while the ST is hydrophilic. In the case of NR-g-ST, the good distribution of light-gray color on the surface of polymer blend (Fig. 4(B)) revealed that NR-g-ST. However, some ST part was poor dispersed in polymer matrix (Fig. 4(B)) indicated the weak interfacial interaction between the polymer matrix (NR-g-ST) and ST. Therefore, NR-g-ST should be selected for coating membrane in encapsulated fertilizer.

3.4. Thermal behavior of NR-g-ST

TGA thermograms of plain NR, plain ST, NR/ST blend and NR-g-ST are presented in Fig. 5. The weight loss of all samples started at 100 °C, which was indicated in the moisture content. A three-stage thermal degradation profile was observed for all samples, the first stage of degradation in plain NR, plain ST, NR/ST blend and NR-g-ST specimens was negligible. The first weight loss stage varied with no specific trend for different compositions. This may be attributed to their residual water content in the network and the remaining acetate functional groups, which are more susceptible for cleavage than the OH functional group (Charoenkul, Uttapap, Pathipanawat, & Takeda, 2011;

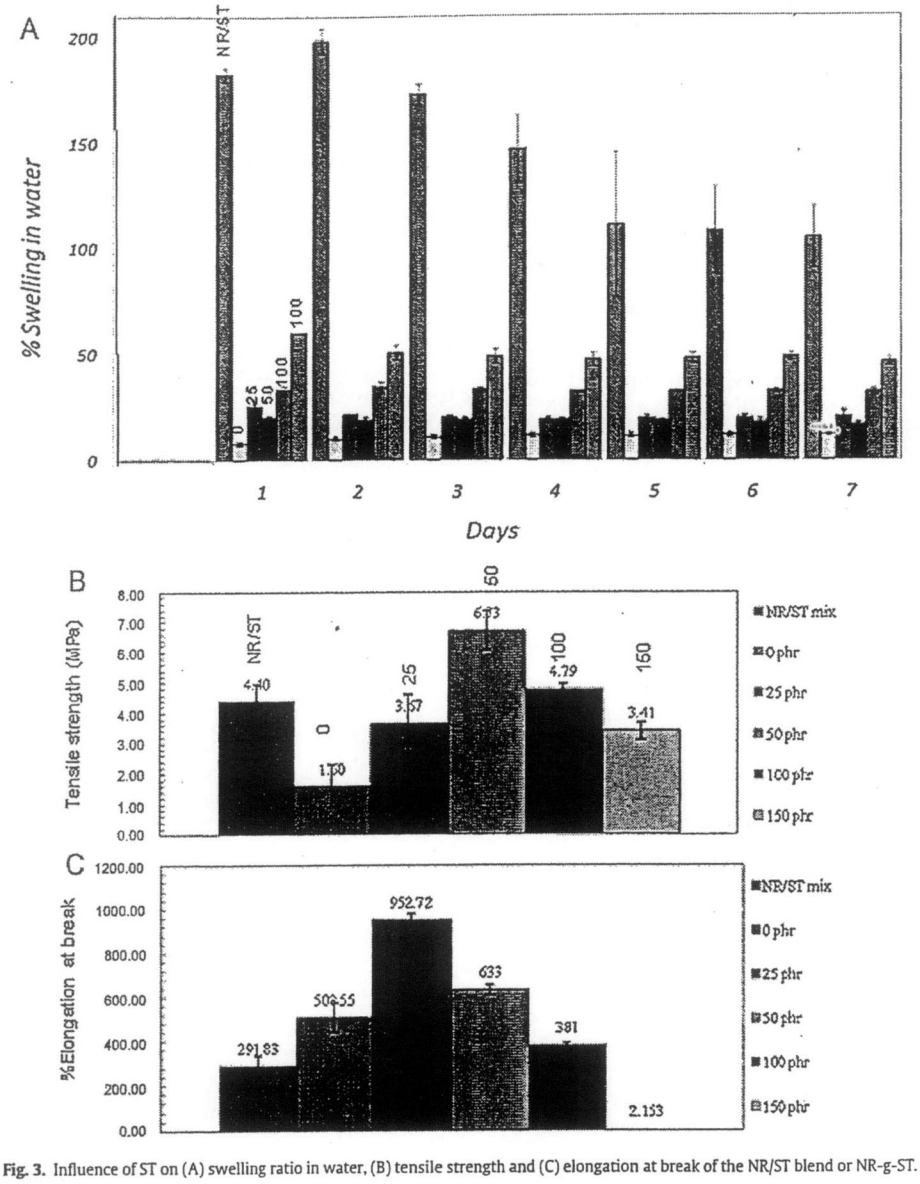

Fig. 3. Influence of ST on (A) swelling ratio in water, (B) tensile strength and (C) elongation at break of the NR/ST blend or NR-g-ST.

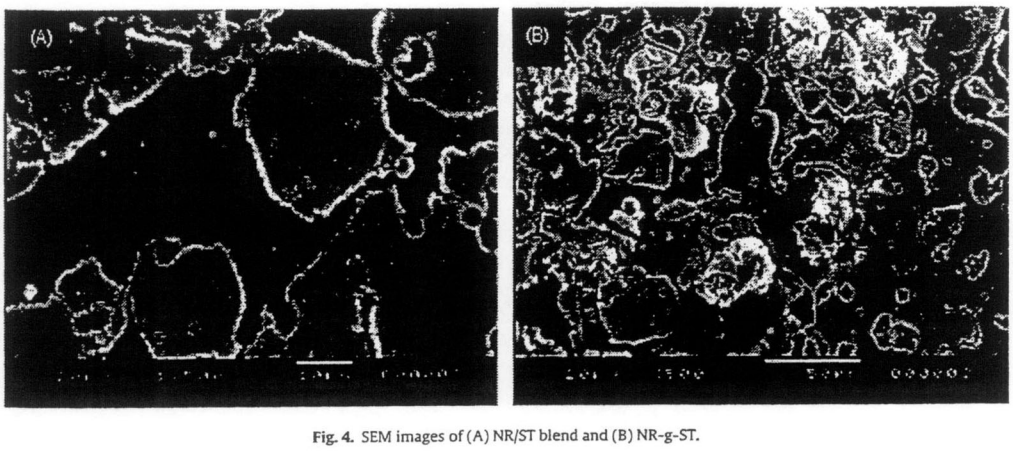

Fig. 4. SEM images of (A) NR/ST blend and (B) NR-g-ST.

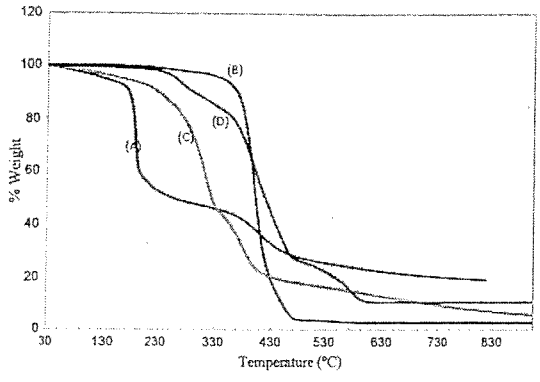

Fig. 5. TGA thermograms of (A) NR, (B) NR/ST blend, (C) NR/$K_2S_2O_8$ and (D) NR-g-ST.

Demiate, Dupuy, Huvenne, Cereda, & Wosiacki, 2000; Parra, Tadini, Ponce, & Lugão, 2004; Sriburi, Hill, & Barclay, 1999). Each sample showed its own temperature range for each stage according to the composition. The overall temperature range for first stage was up to 200 °C, the second stage from 200 to 400 °C and the third stage from 400 up to 600 °C. The thermal degradation process of NR and NR-g-ST were very similar, and there were only one turn in the TG curve (Fig. 5), indicating that the thermal degradation of NR. The thermal degradation curve of modified ST/NR blend, compared to the pristine NR, shifts towards low temperatures, while that of the NR-g-ST moves to higher temperatures at 450–550 °C. The thermal stability of NR was improved significantly after grafting with modified ST (Liu et al., 2008). The enhanced thermal stability and mechanical properties of NR-g-ST were mainly expected due to the improved phase interface interactions between rubber and ST.

3.5. Encapsulation of urea fertilizer

The urea fertilizer granule was surrounded by different walls and released through diffusion in water medium. The amphiphilic NR-g-ST has a core–shell structure with a hydrophobic NR as a core and a hydrophilic grafted ST as a shell. The hydrophobic NR core formed a wall-like barrier inside, while the hydrophilic starch part and the urea particles were encapsulated inside the matrix as shown in as shown in Fig. 6. Urea fertilizer contents

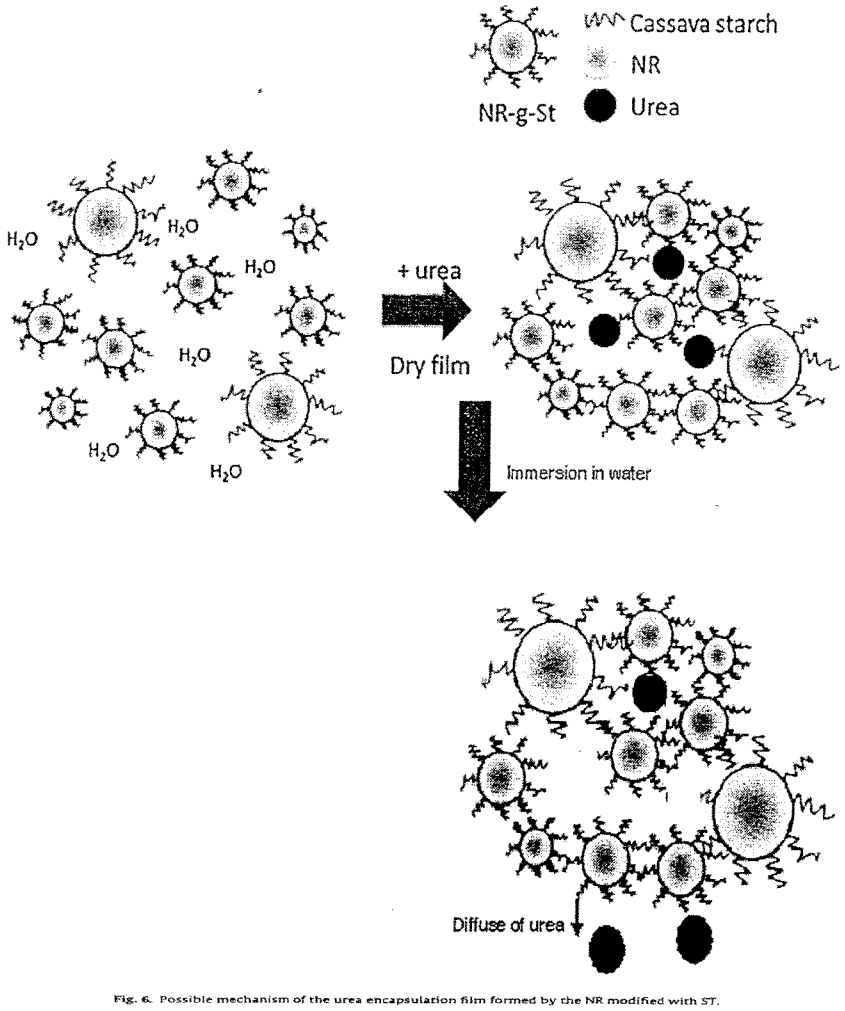

Fig. 6. Possible mechanism of the urea encapsulation film formed by the NR modified with ST.

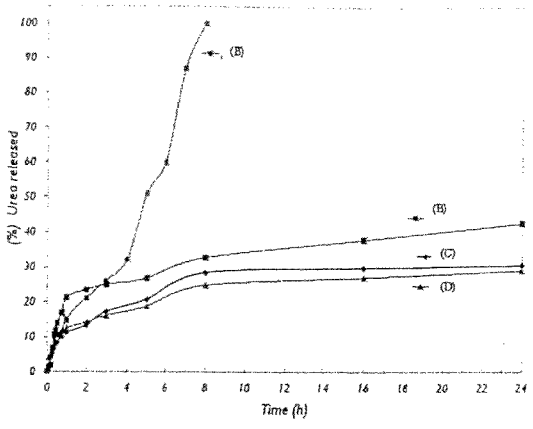

Fig. 7. Urea fertilizer release curves from capsule with coating (A) ST, (B) NR, (C) NR/ST blending and (D) NR-g-ST.

may be released by swelling it under particular conditions, as in the case of an enteric fertilizer coating. In other systems, the wall is broken by solvent action and hydrolysis as shown in Fig. 6.

After water washing, the urea exposed on the surface of bead was removed completely. By measuring urea content in the water, the released urea from capsule was calculated by using UV–vis spectroscopy. The release profile of urea with ST coating was also shown for comparison. The urea release rate was reduced significantly by NR-g-ST coating, which is consistent with the results of the swelling study as shown in Fig. 7. The NR-g-ST membrane is very strong, rigid and hard to swell, thus the diffusion through this coating is the rate limiting step for swelling and urea release. These phenomena may be explained by different swell ability of NR-g-ST matrix because ST and NR/ST can easily be swollen by water. The urea in the swollen NR/ST blend or plain ST can diffuse rapidly and can be released quickly due to weak interaction between urea and polymer matrix membrane. The urea cumulatively release from capsule coating with plain ST was almost complete within 8 h. When NR, NR/ST blend and NR-g-ST coated on capsule, the urea cumulatively release of capsule stored at the same condition for 24 h was 24, 40 and 21%, respectively. With NR-g-ST coating, the capsule matrix becomes denser resulting in a decrease in the rate of diffusion of urea through the swollen beads due to chemical interaction between NR and ST through grafting interaction. This result is supported by Chen et al. (2008). They found that the ST-g-poly(L-lactide) (PLLA) is an effective material for encapsulating urea for controlled release (Chen et al., 2008).

3.6. Biodegradable

The reduction of weight of pristine NR, NR/ST blend and NR-g-ST decomposed in soil was investigated. Results in Fig. 8 display that after chemical modification of NR, the biodegradation of NR-g-ST dramatically increased with increasing the ST contents. The rate of biodegradable of NR-g-ST was faster than that of NR/ST and NR due to grafting between NR and ST. ST was greatly degraded by bacteria and fungi in soil activated by moisture and heat. In the case of NR containing high molecular weight ($\sim 10^6$) a *cis*-1,4-polyisoprene were responsible for the more difficult biodegradation (Bhatt, Shah, Patel, & Trivedi, 2008). The previous work reported that NR can be slowly degraded in nature by specific microorganisms (Bhatt et al., 2008). The high rate of degradation of NR-g-ST within 3 weeks was due to the high amount of ST in the NR-g-ST.

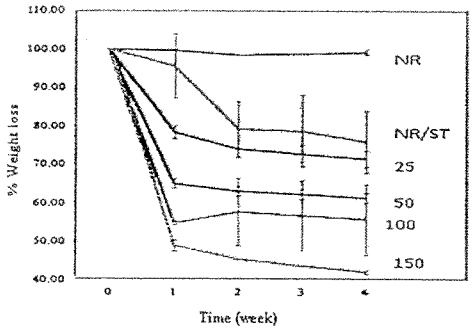

Fig. 8. Weight loss of pristine NR, NR/ST blend and NR-g-ST with different ST contents in soil.

4. Conclusions

The NR-g-ST was achieved to graft with modified ST and $K_2S_2O_8$ as a catalyst for coating the granular fertilizer to reduce solubility in water. The structure modified NR was confirmed by ATR-FTIR. In medium water, the swelling ratio of the modified NR decreased as function of ST due to hydrophilic behavior of ST incorporation in NR matrix. In addition, the tensile strength of modified NR in the presence of ST at 50 phr was the highest compared to other sample and the thermal stability modified NR-g-ST was higher than that of NR-g-ST, which was confirmed by TGA. After NR grafted with ST, it can lead the intermolecular linkage between ST and NR molecules therefore the hydrophobic groups of NR were reduced to control releasing urea fertilizer from capsule. The NR-g-ST membrane displays a good barrier for controlling release of urea fertilizer from capsule and easily degraded in soil. This product with good controlled-release and water-retention could be especially useful in agricultural and horticultural applications.

Acknowledgments

The authors are grateful for the fundamental research grant from The Thailand Research Fund/Commission on Higher Education: Grant No: (MRG5380190) and Prince of Songkla University (SCI 540032S) that supported this work.

References

Abu Bakar, N. H. H., Ismail, J., & Abu Bakar, M. (2010). Silver nanoparticles in polyvinylpyrrolidone grafted natural rubber. *Reactive and Functional Polymers, 70*, 168–174.

Agarwal, K., Setua, D. K., & Sekha, K. (2005). Scanning electron microscopy study on the influence of temperature on tear strength and failure mechanism of natural rubber vulcanizates. *Polymer Testing, 24*, 781–789.

Antoine, R., Luc, R., & Gilbert, R. G. (2004). Synthesis and properties of composites of starch and chemically modified natural rubber. *Polymer, 45*, 7813–7820.

Bhatt, R., Shah, D., Patel, K. C., & Trivedi, U. (2008). PHA-rubber blends: Synthesis, characterization and biodegradation. *Bioresource Technology, 99*, 4615–4620.

Bhatt, R., Shah, D., Patel, K. C., Trivedi, U., Carvalhoa, A. J. F., Job, C. E., et al. (2003). Thermoplastic starch/natural rubber blends. *Carbohydrate Polymers, 53*, 95–99.

Carvalhoa, A. J. F., Jobb, A. E., Alvesb, N., Curveloa, A. A. S., & Gandini, A. (2003). Thermoplastic starch/natural rubber blends. *Carbohydrate Polymers, 53*, 95–99.

Chaikumpollert, O., Sae-Heng, K., Wakisaka, O., Mase, A., Yamamoto, Y., & Kawahara, S. (2011). Low temperature degradation and characterization of natural rubber. *Polymer Degradation and Stability, 96*, 1989–1995.

Charoenkul, N., Uttapap, D., Pathipanawat, W., & Takeda, Y. (2011). Physicochemical characteristics of starches and flours from cassava varieties having different cooked root textures. *LWT - Food Science and Technology, 44*, 1774–1781.

Chiu, P. E., & Lai, L. S. (2010). Antimicrobial activities of tapioca starch/decolorized hsian-tsao leaf gum coatings containing green tea extracts in fruit-based salads, romaine hearts and pork slices. *International Journal of Food Microbiology, 139*, 23–30.

Chen, L., Xie, Z., Zhuang, X., Chen, X., & Jing, X. (2008). Controlled release of urea encapsulated by starch-g-poly(L-lactide). *Carbohydrate Polymers, 72*, 342–348.

Demiate, I. M., Dupuy, N., Huvenne, J. P., Cereda, M. P., & Wosiacki, G. (2000). Relationship between baking behavior of modified cassava starches and starch chemical structure determined by FTIR spectroscopy. *Carbohydrate Polymers, 42*, 149–158.

Derouet, D., Intharapat, P., Tran, Q. N., Gohier, F., & Nakason, C. (2009). Graft copolymers of natural rubber and poly(dimethyl-(acryloyloxymethyl) phosphonate) (NR-g-PDMAMP) or poly(dimethyl(methacryloyloxyethyl) phosphonate) (NR-g-PDMMEP) from photo-polymerization in latex medium. *European Polymer Journal, 45*, 820–836.

Gan, S. N., & Hamid, Z. A. (1997). Partial conversion of epoxide groups to diols in epoxidized natural rubber. *Polymer, 38*(8), 1953–1956.

Kim, Y. K., Mukerjea, R., & Robyt, J. F. (2010). Controlled release of D-glucose from starch granules containing 29% free D-glucose and Eudragit L100-55 as a binding and coating agent. *Carbohydrate Research, 345*, 1065–1067.

Kongparakul, S., Prasassarakich, P., & Rempel, G. L. (2008). Catalytic hydrogenation of methyl methacrylate-g-natural rubber (MMA-g-NR) in the presence of $OsHCl(CO)(O_2)(PCy_3)_2$. *Applied Catalysis A: General, 344*, 88–97.

Lanthong, P., Nuisin, R., & Kiatkamjornwong, S. (2006). Graft copolymerization characterization, and degradation of cassava starch-g-acrylamide/itaconic acid superabsorbents. *Carbohydrate Polymers, 66*, 229–245.

Liu, C., Shao, Y., & Jia, D. (2008). Chemically modified starch reinforced natural rubber composites. *Polymer, 49*, 2176–2181.

Mahittikul, A., Prasassarakich, P., & Rempel, G. L. (2009). Hydrogenation of natural rubber latex in the presence of $[Ir(cod)(PC_{y3})(py)]PF_6$. *Journal of Molecular Catalysis A: Chemical, 297*, 135–141.

Parra, D. F., Tadini, C. C., Ponce, P., & Lugão, A. B. (2004). Mechanical properties and water vapor transmission in some blends of cassava starch edible films. *Carbohydrate Polymers, 58*, 475–481.

Pasquini, D., Teixeira, E. D. M., Curvelo, A. A. D. S., Belgacem, M. N., & Dufresne, A. (2010). Extraction of cellulose whiskers from cassava bagasse and their applications as reinforcing agent in natural rubber. *Industrial Crops and Products, 32*, 486–490.

Riyajan, S. (2007). Swell behavior affecting degradation of purified natural rubber. *Kaustschuk Gummi Kunststoffe, 60*, 94–100.

Rouilly, A., Rigal, L., & Gilbert, R. G. (2004). Synthesis and properties of composites of starch and chemically modified natural rubber. *Polymer, 45*, 7813–7820.

Sriburi, P., Hill, S. E., & Barclay, F. (1999). Depolymerisation of cassava starch. *Carbohydrate Polymers, 38*, 211–218.

Tanrattanakul, V., & Chumeka, W. (2010). Effect of potassium persulfate on graft copolymerization and mechanical properties of cassava starch/natural rubber foams. *Journal of Applied Polymer Science, 116*, 93–105.

Valodkar, M., & Thakore, S. (2011). Organically modified nanosized starch derivatives as excellent reinforcing agents for bionanocomposites. *Carbohydrate Polymers, 86*, 1244–1251.

Wang, Z.-F., Peng, Z., Li, S.-D., Lin, H., Zhang, K.-X., She, X.-D., et al. (2009). The impact of esterification on the properties of starch/natural rubber composite. *Composites Science and Technology, 69*, 1797–1803.

Yu, H., Zeng, Z., Lu, G., & Wang, Q. (2008). Processing characteristics and thermal stabilities of gel and sol of epoxidized natural rubber. *European Polymer Journal, 44*, 453–464.

Zhi-Fen, W., Zheng, P., Si-Dong, L., Hua, L., Ke-Xi, Z., Xiao-Dong, S., et al. (2009). The impact of esterification on the properties of starch/natural rubber composite. *Composites Science and Technology, 69*, 1797–1803.

Zou, W., Yu, L., Liu, X., Chen, L., Zhang, X., Qiao, D., et al. (2012). Effects of amylose/amylopectin ratio of starch-based superabsorbent polymers. *Carbohydrate Polymers, 87*, 1583–1588.

Zou, W., Yu, L., Liu, X., Chen, L., Zhang, X., Qiao, D., et al. (2001). Synthesis and properties of natural rubber modified with stearyl methacrylate and divinylbenzene by graft polymerization. *Journal of Applied Polymer Science, 79*(13), 2464–2470.

J Polym Environ
DOI 10.1007/s10924-012-0510-x

ORIGINAL PAPER

Chemical Crosslink Degradable PVA Aqueous Solution by Potassium Persulphate

Sa-Ad Riyajan · Yodsathorn Sasithornsonti

Author Proof

Abstract The aim of this paper is to study the influence of the $K_2S_2O_8$ content on the properties Poly (vinyl alcohol, (PVA). Firstly, PVA was dissolved in distilled water by heating by heating at 70 °C and then $K_2S_2O_8$ was added in PVA solution under stirrer. The viscosity of PVA solution in the presence of $K_2S_2O_8$ was analyzed by Brookfield Viscometers. The effects of $K_2S_2O_8$ contents, PVA solution, temperature and reaction time on the viscosity of PVA solution were investigated. This was confirmed by Brookfield Viscometers. It is clear that the viscosity of PVA solution in the presence of $K_2S_2O_8$ increased as function of reaction time and PVA content in solution. Rate of modified PVA was proportional to $K_2S_2O_8$ contents and temperature and its activation energy was 16 kJ/mol. The structure of PVA in the presence of $K_2S_2O_8$ changed from original PVA confirmed by ATR-FTIR and solid state NMR. In addition, the thermal properties of PVA containing $K_2S_2O_8$ were also studied by TGA.

Keywords Poly (vinyl alcohol) · Activation energy · Potassium persulfate · Viscosity

Introduction

Poly (vinyl alcohols), (PVA) is widely used in industrial fields because its advantages are water-soluble polymer, biodegradable polymer and low toxic. The chemical modification has subsequently applied to improve the properties of PVA, leading to many applications of PVA, especially made in polymer hydrogel. In previous work, the degradation method of PVA are thermal degradation [1–3], radiation [4], ultrasonic [5], mechanical [6], biodegradation [7–10], photodegradation [11–14], and chemical degradation [15, 16]. For example about degradation of PVA, gamma rays introduced the degradation of PVA alone through chain scission and cyclization observing formation of C = C and C = O bonds. But when adding humic acids of concentration 0.5–10 % in the PVA sample, PVA showed the good degradation resistance [12]. In case of ultrasonic, it can yield polymer degradation as observed from a significant reduction in the intrinsic viscosity or the molecular weight. The main factors affecting on the degradation of PVA by this ultrasonic method are irradiation time, immersion depth of horn and PVA concentration. The viscosity of polymer solution decreased with an increase in the ultrasonic irradiation time and approached a limiting value. In addition, the air, sodium chloride and surfactant enhances in increasing the extent of viscosity reduction. In addition, the oxidative degradation of PVA by the photochemically enhanced Fenton reaction was studied using a mixture of Fe^{2+}_{aq} and H_2O_2) and a heterogeneous reaction system (iron (III)-exchanged zeolite Y + H_2O_2) [17]. Results showed that the formation of super-macromolecules (MW: 1–5 × 10^6 g/mol) consisting of oxidized PVA and trapped iron (III) at an early reaction stage. During the heterogeneous Fenton process, the cleavage of the PVA-chains may occur at random positions, the reactive centers being located inside the iron (III)-doped zeolite Y photocatalysts. In the previous work, the chemical degradation of PVA was severally reported. However, the chemical degradation of PVA by using $K_2S_2O_8$ as a catalyst has not yet been reported. The benefits of chemical degradation of PVA in the presence of $K_2S_2O_8$ are expected to a coating agent membrane for encapsulated reactive agent or

S.-A. Riyajan (✉) · Y. Sasithornsonti
Department of Materials Science and Technology,
Faculty of Science, Prince of Songkla University,
Songkhla 90112, Thailand
e-mail: saadriyajan@hotmail.com

Table 1 Influence of the reaction time on dynamic viscosity of PVA (a) with in (b) without 5 % w/w $K_2S_2O_8$at 70 °C

$K_2S_2O_8$ (g)	%Relative dynamic viscosity from original viscosity (cps)							
	0 min	6 min	10 min	20 min	30 min	40 min	50 min	60 min
0	20	35	65	70	80	85	91.5	97.5
1	13	38	56	98	385	gel at 32 min		

Fig. 1 Photograph of modified PVA with in 5 % w/w $K_2S_2O_8$ at 70 °C at 32 min

continued to 30 min as shown in Fig. 1. This phenomenon was called "gel" and this result was explained that after $K_2S_2O_8$ is activated with heat, it gave the free-radical form. Then, it reacts with PVA molecule. After that, the PVA molecule occurred chain scission and at same time short PVA reacted together to crosslinkaged PVA through ether linkages leading to very high dynamic viscosity of PVA [4]. The detail mechanism of PVA added $K_2S_2O_8$ was explained in section "Effect of $K_2S_2O_8$ on dynamic viscosity of PVA".

Effect of $K_2S_2O_8$ on Dynamic Viscosity of PVA

The influence of $K_2S_2O_8$ content on the dynamic viscosity of PVA was presented in Fig. 2. It is clear that the dynamic viscosity of PVA increase with increasing $K_2S_2O_8$ and reaction time. The reaction time to gel point of PVA

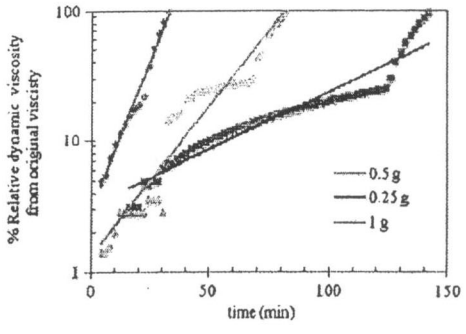

Fig. 2 Influence of the temperature (*a*) 50, (*b*) 70 and (*c*) 90 °C on the viscosity of PVA modified with $K_2S_2O_8$

decrease after higher amount of $K_2S_2O_8$ was added to PVA solution. When 0.25, 0.5 and 1.0 g $K_2S_2O_8$ were added to PVA, the reaction time to gel point (three dimensional crosslinking) of PVA was 140, 82 and 32 min, respectively. This result was explained that when more amount of $K_2S_2O_8$ was added to PVA, the more radical was found and it leaded to decrease in reaction time to gel point.

Effect of PVA Concentration on Dynamic Viscosity of PVA

Figure 3 shows the influence of %PVA concentration on its dynamic viscosity. Results showed that, the reaction time to gel content increase with increasing PVA concentration. The reaction time to gel point of 2.5, 5, 10 and 15 w/w % of PVA solution was 4, 8, 32 and 74 min, respectively. When PVA molecule increased in system but the

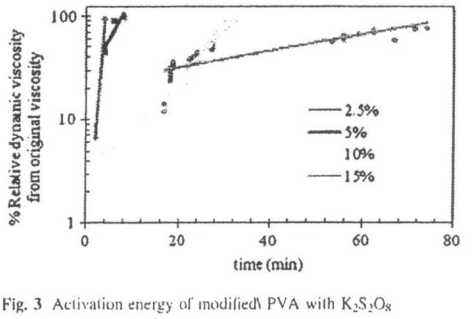

Fig. 3 Activation energy of modified\ PVA with $K_2S_2O_8$

Journal Large 10924 | Dispatch 21-7-2012 | Pages 7
Article No. : 510 | LE | TYPESET
MS Code : JOOE-859 | CP | DISK

concentration of $K_2S_2O_8$ was constant. Therefore, the free radical content was not enough to react with PVA molecule leading to increase in reaction time to gel point [1].

Effect of Temperature on Dynamic Viscosity of PVA

The influence of temperature on the dynamic viscosity of PVA was shown in Fig. 4. It is clear that the dynamic viscosity of PVA decreased as a function of temperature. If the dynamic viscosity of PVA at 323, 343 and 363 K, the reaction time to gel point was 102, 32 and 6 min, respectively. If the temperature increased, the rate of free radical occurs dramatically, leading to higher gel formation. In addition, as the temperature increases, the activation energy of the degraded PVA decreased. Therefore, the reaction time to gel point of PVA decreased as a function of temperature.

Kinetic Study

The model-free kinetics is based on calculation of the effective activation energy (E_a) as a function of the conversion (α) of a chemical reaction $E = f(\alpha)$. A chemical reaction is measured at least three different heating rates (β) and the respective conversion curves are calculated out of the TG measured curves. For each conversion (α) ln β/T^2 is plotted versus $1/T_\alpha$ giving rise to a straight line with slope—$E_{a\alpha}/R$, therefore providing the activation energy as a function of conversion [19]. The activation energy results of modified PVA are displayed in Fig. 5. It was found that, the activation energy of PVA was about16 kJ/mol at regression of 99.41 %.

Swelling Ratio Results

The effect of $K_2S_2O_8$ on swelling ratio of PVA was shown in Fig. 6. The crosslinking of PVA through etherification at hydroxyl group from PVA was further confirmed through swelling experiments. These results showed that, the swelling ratio of PVA decreased with increasing $K_2S_2O_8$. The swelling ratio of PVA in the presence of 0.25, 0.5, 1, 2.5 and 5 % w/w $K_2S_2O_8$ was 105, 130, 420 and 910 %, respectively. This results was explained that the high crosslinking density of PVA in the presence of high amount of $K_2S_2O_8$ after chemical modification and rearrangement of PVA molecule.

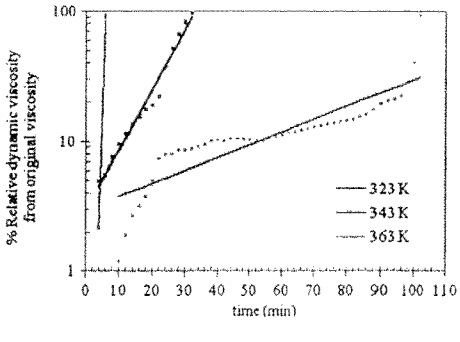

Fig. 4 Influence of the potassium persulphate on the viscosity of PVA with $K_2S_2O_8$ (*a*) 2.5 %, (*b*) 5 %, (*c*) 10 % and (*d*) 20 % w/w

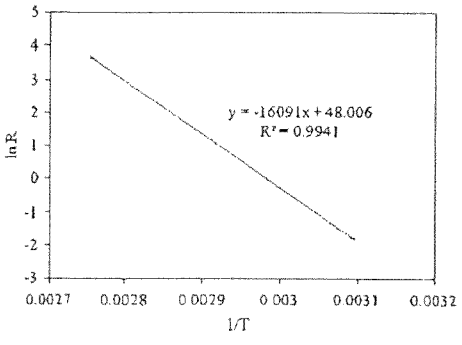

Fig. 5 Effect of PVA concentration (*a*) 2.5 %, (*b*) 5 %, (*c*) 10 % and (*d*) 15 % w/w on the dynamic viscosity of PVA with 5 % w/w $K_2S_2O_8$ at 70 °C

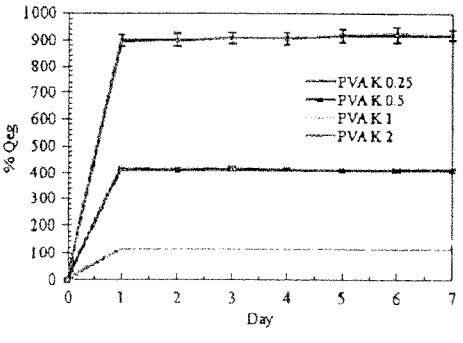

Fig. 6 Swelling of modified PVA with $K_2S_2O_8$

FTIR Spectra

The possible mechanism of degradation of PVA by using potassium persulphate is presented in Fig. 7. The potassium persulphate was activated by heat and then changed free radical. The potassium persulphate free radical reacted with hydroxyl group from PVA to get the PVA free radicals form. After that, the PVA free radicals continued to react with together and gave the crosslinking product as a predominat component as shown in Fig. 7. At the same

Journal : Large 10924 | Dispatch : 21-7-2012 | Pages : 7
Article No. : 510 | LE | TYPESET
MS Code : JOQE-859 | CP | DISK

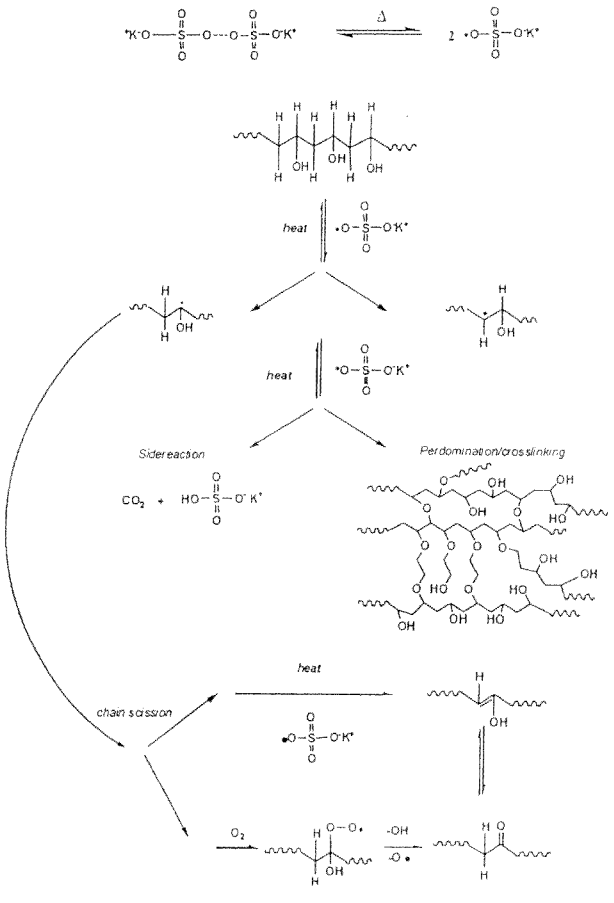

Fig. 7 Possible mechanism of modified PVA with $K_2S_2O_8$

time, in cases where considerable elimination of hydroxyl groups has already occurred, such reactions may only lead to random scission and liberate unsaturated aldehydes and ketones. Then, it reacts with PVA molecule. After that, the PVA molecule occurred chain scission and at same time short PVA reacted together to crosslinkaged PVA through ether linkages leading to very high dynamic viscosity of PVA [4].

Figure 8 shows the ATR-FTIR spectra of unmodified and modified PVA. It was found that the chemical structure of PVA altered after addition of $K_2S_2O_8$ in PVA solution. The main peak of PVA was observed at 3450, 2930, 2050, 1750, 1640, 1585, 1427, 1331, 1140, 1094 and 916 cm^{-1}. The peak at 1427 cm^{-1} is designated to the CH_2 scissoring mode and the peaks at 1375 and 1331 cm^{-1} are attributed to CH_2 deformation. In addition, C–O and C–C stretching vibration peaks appear at 1094 and 916 cm^{-1}, respectively. The peak at 850 cm^{-1} was associated with the CH_2 rocking mode of PVA. Notably, the peak at 1140 cm^{-1}, which is related to crystalline C–O stretching vibration, strongly depends on the degree and rate of crystallization of the PVA matrix [17]. In addition, the deconvoluted peaks for amorphous PVA and modified PVA in the range of 1160–970 cm^{-1} are shown in Fig. 7. The band at 2930 cm^{-1} is clearly associated with saturated C–H stretching which when considered in conjunction with the relatively low intensity of the conjugation band at 1585 cm^{-1} compared to the solid residue of PVA. Three peaks at 1125, 1094, and 1055 cm^{-1} are attributed to C–O stretching vibration of saturated alcohol, and the deconvoluted peaks were located at similar positions in both cases. It is noteworthy that the crystalline C–O–C stretching peak at 1140 cm^{-1} (Fig. 8 (b) and (c)) does not appear in the case of pristine PVA. When modified PVA was heated from 50 to 300 °C by TGA, the residue PVA was characterized by

Journal : Large 10924 | Dispatch : 21-7-2012 | Pages : 7
Article No. : 510 | LE | TYPESET
MS Code : JOOE-859 | CP | DISK

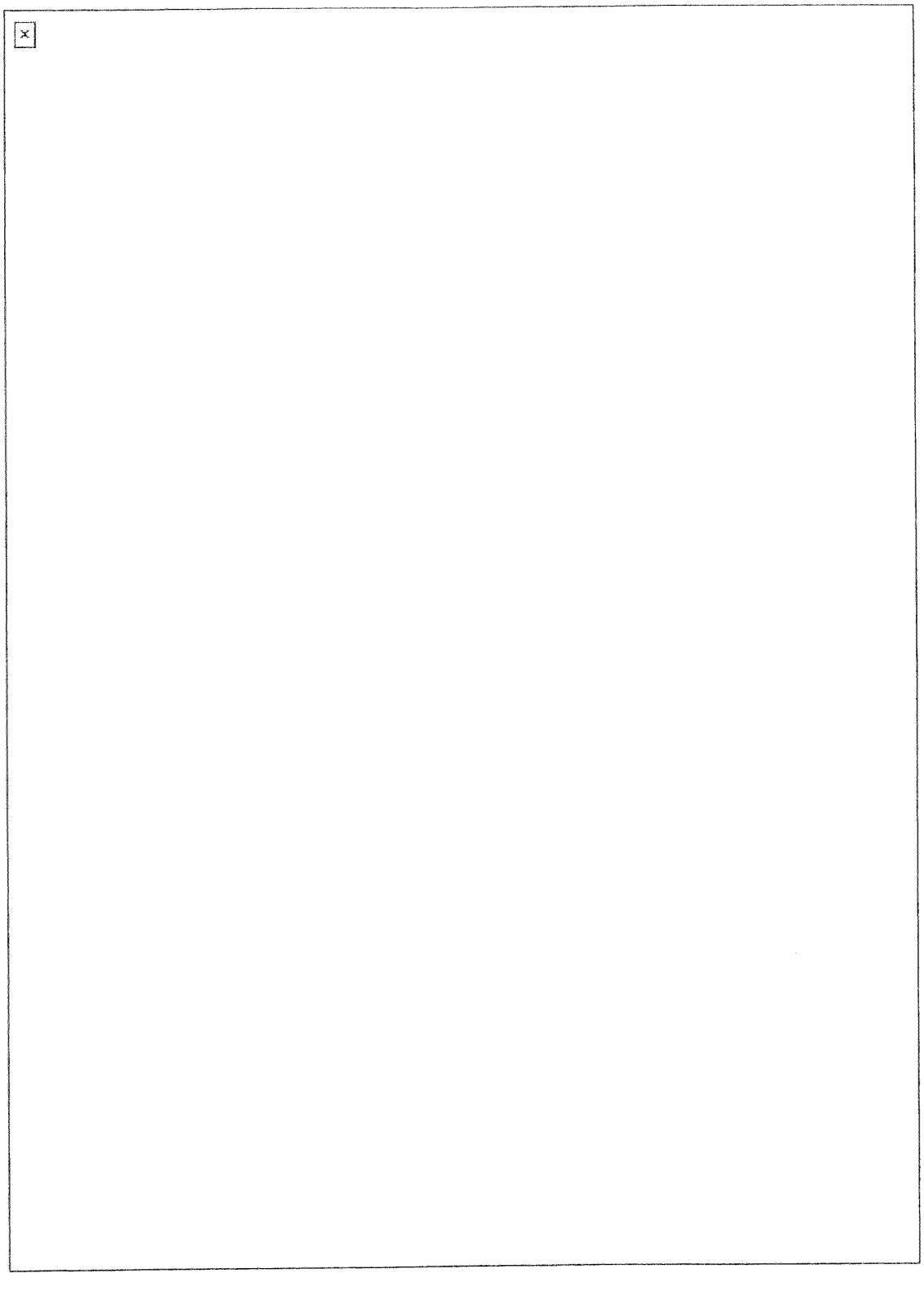

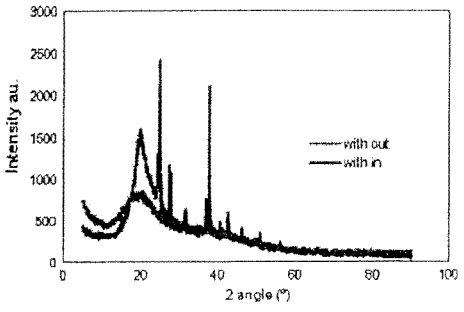

Fig. 10 TGA thermographs of (*a*) pristine PVA and (*b*) crosslinked PVA

600 °C. The second phase is accompanied with a physical phenomenon such as melting of crystallites followed by degradation of PVA at 200–400 °C.

The heat required for melting of 100 % crystalline PVA is 138.6 J/g [19]. Therefore, the degree of crystallinity can be quantitatively estimated by the enthalpy of melting, which is the second relaxation in the temperature range of 200–250 °C. The third stage from 400 °C up to 600 °C. Comparing before and after chemical modification, the stability of modified PVA at third period was higher than that of unmodified PVA at 300–700 °C but at 200–300 °C the thermal stability of unmodified PVA was higher than that of modified PVA due to occurrence of PVA chain scission. It was explained that pseudo-crosslinking due to the induced crystallinity in PVA itself can improve its thermal stability [18]. The maximum decomposition temperature of PVA shifted significantly from about 300 °C to about 700 °C after the PVA was treated with $K_2S_2O_8$. It can be concluded that the thermal stability of modified PVA increases due to crosslinking product through ester linkage at hydroxyl group from PVA molecules. The heat required for melting of 100 % crystalline PVA is 138.6 J/g [12]. Therefore, the degree of crystallinity can be quantitatively estimated by the enthalpy of melting, which is the third relaxation in the temperature range of 200–250 °C.

Conclusions

The viscosity of PVA increased as a function of the $K_2S_2O_8$ content, temperature and reaction time analyzed by Brookfield Viscometers. The activation energy of modified PVA with $K_2S_2O_8$ was found to be 16.5 kJ/mol and regression at 99.41 %. The chemical structure of modified PVA with $K_2S_2O_8$ changed from original PVA confirmed by ATR-FTIR and solid state of NMR due to crosslinking formation. The swelling ratio of PVA decreased with increasing $K_2S_2O_8$. In addition, the thermal properties of modified PVA were enhanced after chemical modification. The resulting material will be used in medical or agriculture application in further due to crosslinking formation of PVA.

Acknowledgments The authors thank the polymer science Program, Faculty of Science, Prince of Songkla University for the use of laboratory space. This study was supported by The Thailand research fund (MRG5380190) and the Prince of Songkla University (SCI 540032S).

References

1. Holland BJ, Hay JN (2001) Polymer 42:6775
2. Peng Z, Long LX (2007) Polym Degrad Stabil 92:61
3. Baimuratov E, Saidov DS, Kalontarov IY (1993) Polym Degrad Stabil 9:35
4. Shu-Juan Z, Han-Qing Y (2004) Water Res 38:309
5. Mohod Ashish V, Gogate Parag R (2011) Ultrason Sonochem 18:727
6. Shara F, Mansour SA, El-Lawindy AMY (1999) Polym Degrad Stabil 66:173
7. Takasu A, Itou H, Takada M, Inai Y, Hirabayashi T (2002) Polymer 43:227
8. Yujian W, Xiaojuan Y, Hongyu L, Wei T (2006) Polym Degrad Stabil 91:2408
9. Emo C, Andrea C, Roberto S (1999) Polym Degrad Stabil 4:305
10. Andrea C, Roberto S, Emo C (2002) Polym Degrad Stabil 75:447
11. Giroto JA, Guardani R, Teixeira ACSC, Nascimento CAO (2006) Chem Eng Process 45:523
12. Gongxu L, Hongying C, Dongyuan L (1993) Radiat Phys Chem 42:229
13. Yingxu C, Zhenshi S, Ye Y, Qiang K (2001) J Photochem Photobiol, A 142:85
14. Mawada D, Penny Martensa J, Ross Odella A, Laura Poole-Warren A (2007) Biomaterials 28:947
15. Congming X, Gaoyan Z (2003) Polym Degrad Stabil 81:297
16. Bossmann SH, Oliveros E, Göb S, Kantor M, Göppert A, Lei L, Yue PL, Braun AM (2001) Braun Water Sci Technol 44:257
17. Lai S, Casu M, Saba G, Lai A, Husu I, Masci G, Crescenzi V (2002) Solid State Nucl Magn Reson 21:187
18. Krklješ AN, Marinović-Cincović MT, Kačarević-Popović ZM, Nedeljković JM (2007) Thermochim Acta 460:28
19. Liu Y, Geever LM, Kennedy JE, Higginbotham CL, Cahill PA, McGuinness GB (2010) J Mech Behav Biomed 3:203

Journal : Large 10924 | Dispatch : 21-7-2012 | Pages : 7
Article No. : 510 | LE | TYPESET
MS Code : JOOE-859 | CP | DISK